ECRONICON OPEN ACCESS

EC ORTHOPAEDICS
Research Article

Evaluation of Lower Limb Injury against AP Mine Blast: Numerical and Experimental Trials

Mehmet Karahan* and Nevin Karahan

Vocational School of Technical Sciences, Bursa Uludag University, Görükle-Bursa, Turkey

***Corresponding Author:** Mehmet Karahan, Vocational School of Technical Sciences, Bursa Uludag University, Görükle-Bursa, Turkey.

Received: February 08, 2020; **Published:** March 23, 2020

Abstract

In this study, the effectiveness of blast deflectors used in protective footwear against AP mines was investigated. The tip-angle of a V-shaped deflector and the overall shape (symmetrical, unsymmetrical) were chosen as the design parameters to be examined, whereas parameters such as deflector material and wall thickness were kept constant. Both explicit dynamic finite element analysis (LS-Dyna) and blasts tests were performed to evaluate the effectiveness of these design parameters. The analysis results were also verified with the blast tests. A visual (qualitative) comparison between the analysis results and blast tests show a good agreement on the final deformed geometry of the deflector, which suggests the simulation was able to capture the energy absorption mechanism of the deflector. The analysis results show that the peak force transmitted to the leg decreases tremendously with the addition a blast deflectors. When compared to the case with no deflectors, an unsymmetrical and symmetrical deflector reduced the peak force by a factor of 24 and 36, respectively.

Keywords: *AP Mine; Protective Boots; Deflector*

Introduction

It is well known that anti-personnel (AP) landmines are a worldwide problem affecting many countries. Despite the recent attempts to prohibit the usage of these weapons, there are still a large number of landmines on the field and stockpiled which pose a constant threat to soldiers and civilians alike.

Even after years of research, no simple approach has been developed for protection against AP landmines due to the extreme loading which induces multiple damage mechanisms on lower body. Main aim of the protective boots or footwear against the landmines is to prevent the loss of victim's foot, but if the damages are irreversible and traumatic amputation is necessary, to keep the amputated area as low as possible. From wearer's perspective the protective boots, must be light and comfortable enough for operational use. More recently, textile structures produced with high performance fibers are being used as reinforcement in the sole of footwear. The majority of these footwear rely on a combination of ballistic composites such as Aramid, Ultra High Molecular Weight Polyethylene (UHMWPE), honey-combed lightweight metals (to absorb or deflect blast). There are also designs that keep the feet off of the ground to increase the standoff distance, thus decreasing the effect of the blast wave.

The design of protective footwear against AP mines requires a specialized material design. The most widely used material in such applications are fiber reinforced composites like Kevlar or Dyneema, which can absorb the blast and provide enough ballistic strength to minimize any secondary shrapnel effect.

There are a few successful application of anti-mine boots available in the industry. "Spider Boot" developed in order to protect against AP mines is a commercialized design [1-3]. This boot keeps the foot above the ground at a particular height. The pods of the boot press the ground away from the projection of the foot, which prevents the blast to be directly below the foot. However, walking with these boots is difficult and running is almost impossible. A long period usage is not a possibility due to lack of mobility and comfort.

The boots which are known as "Over Boots" are worn over a normal or a protective boot. This design keep the feet above the ground by the thickness of boot sole [4,5]. It is not suitable for long period usage again due to the lack of mobility.

More recent studies on protective boots generally focus on designs that look like a conventional army personnel boot. The early designs were reinforced with a metal plate in their sole [6,7]. However, the existence of metal plate reduces the flexibility of the sole and increases the weight of the boot. Later studies have developed lighter constructions by using Kevlar and Dyneema fabric layers with light metal alloys [8-10]. The ones built without using any metal reinforcement had multiple layers of Kevlar and Dyneema composite plates [11-14]. But in these designs, sole of the boot was not flexible because of the stiff composite layers. One of the commercially successful models developed by Zeman Company, included Kevlar layers in the sole which provides protection to a maximum 50 grams of AP mine [15,16]. All of these studies show that, protective capability of the composite layers is limited as the transmitted force, which directly relates to the consequent injury, cannot be lowered by increasing the composite thickness or using high strength fibers due to low compressibility under impulsive loads. Latest designs, therefore, have an energy absorbing media below the composite layers to decrease the magnitude of the incident wave simply by inelastic deformation [17-19]. Such parts are generally in the form of V-shaped deflector in the sole to reflect the incident blast wave, hence reduce the momentum transmitted to the feet [20].

This article focuses on the optimization of a deflector design using explicit finite element simulations performed in Ls-Dyna and the subsequent validation with blast tests.

Sole and deflector design

Using results and calculations of past studies mentioned above, a V-shaped deflector was designed to be embedded in the sole in order to deviate and absorb blast loading. A standard army personnel boot (male EU size 42) was considered to determine the gross dimensions of the deflector. Fiber reinforced composite plates which were cut in the form of the sole, was placed above the deflector to keep the burned soil, shrapnel and deflector (accelerated by the blast loading) away from the foot.

Geometric design of the deflector controls many parameters regarding protective capability. As the tip angle of the V- Shaped deflector increases, the angle of incidence of the blast wave on the inclined surface increases which leads to higher impulse per unit area, i_n, on these surfaces. However, as total impulse can be obtained directly by the integration of i_n over the surface, the surface area facing the impulsive loading is also a critical parameter.

In this study, as the area of the foot sole (a) is constant, decreasing the tip angle (r) leads to an increase in the surface area (S) of deflector (Figure 1) which may result higher momentum being transferred from the blast. Besides, higher tip angle causes lower standoff distance which is another parameter used in impulse formulation. Due to these three conflicting effects of the tip angle, parametric study was needed to determine the most efficient geometry. In addition to the tip angle, a change in the total impulse can also be achieved by shifting the tip of the deflector to a side, so that only one surface is subjected to the blast wave as seen in figure 2.

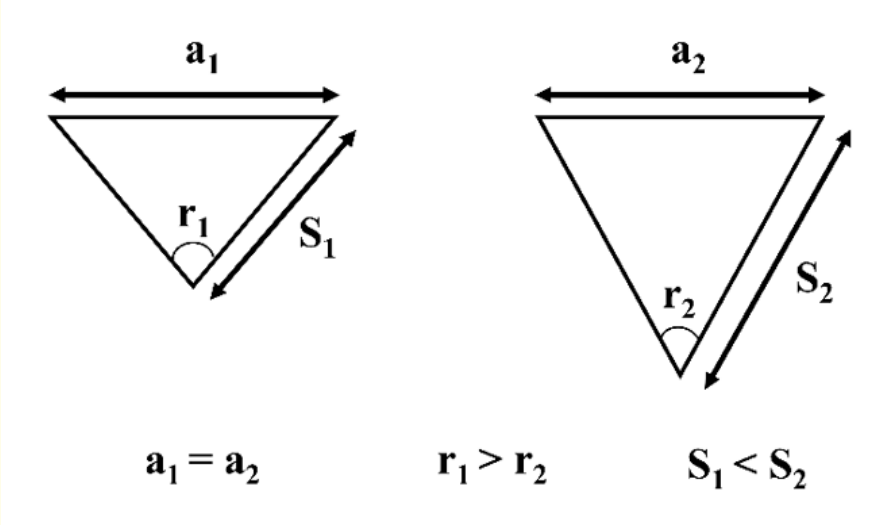

Figure 1: *Effect of change in tip angle (r) on cross section of the deflector.*

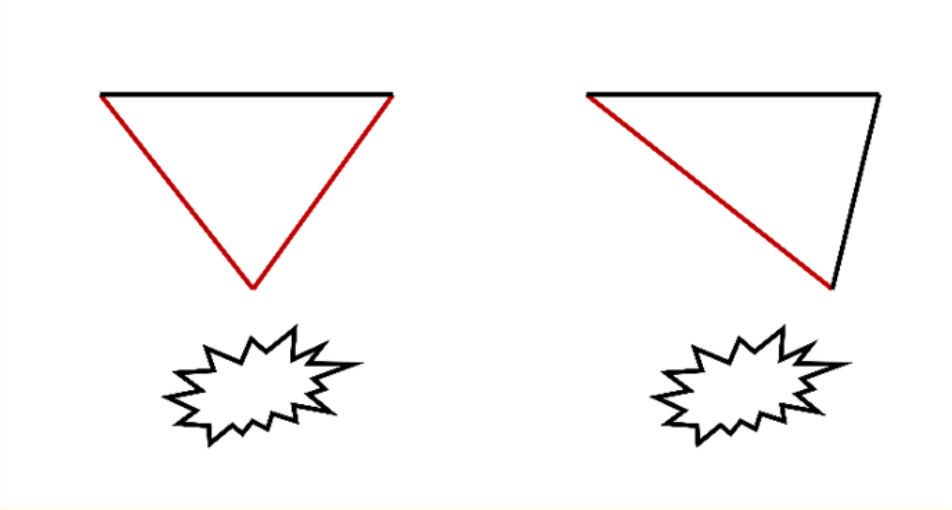

Figure 2: *Surfaces of the deflector exposed to blast loading (in red) for symmetrical and unsymmetrical designs.*

Although, protective performance of the deflector is the primary consideration of the study, practical use and ergonomic properties of the boot should also be considered. As the sole surface area is kept constant in this study, lower tip angle increases the height of the deflector and hence the height of the sole, which seriously limits the mobility of the wearer. A maximum deflector height of 2.5 cm is considered as a constraint in determining the limits of the tip angle varied in numerical parametric studies.

In addition to its geometry, deformation behavior of the deflector is also critical for the protection capability of the boot. As the total impulse (integration of force over time) on the deflector depends on its geometry, lowering force can be achieved by increasing time of exposure, which can be obtained by using low-stiffness material with high compressibility. Hence, the peak force transmitted to the composite layers above the deflectors can be decreased by increasing the amount of material that can absorb energy through inelastic deformation. However, low stiffness brings back low strength that causes localized failure which allows inhomogeneous load transfer. This problem can be hindered by high-strength thin plate covering a deformable core. High stiffness of the plate distribute the blast wave into the deformable, low-stiffness core, so that the entire volume faces a homogeneous compression throughout. Such a mechanism improve the efficiency of the core and delay the load transmitted to the composite layer. Although the selection of the deflector material affects the energy absorption mechanism, it is outside the scope of this work and can be studied separately.

In this study, ANSYS LS-Dyna code was used for numerical analysis. The runs are performed parametrically to investigate the effect of the angle of incidence. Design with shifted-tip (or unsymmetrical design) was also simulated for comparison and experimental blast tests were carried out for qualitative verification.

General appearance of the boots that were used in the tests are shown in figure 3. As can be seen, the boot sole consists of two layers. The bottom part includes an embedded deflector in order to deviate the shockwave. The top part consists of the composite insert plates. In this study, the characteristics of the composite insert layers were kept constant, while the geometry of the deflector was changed. The upper parts of the boot is strengthened with 2-plies of woven fabric aramid between the lining and leather.

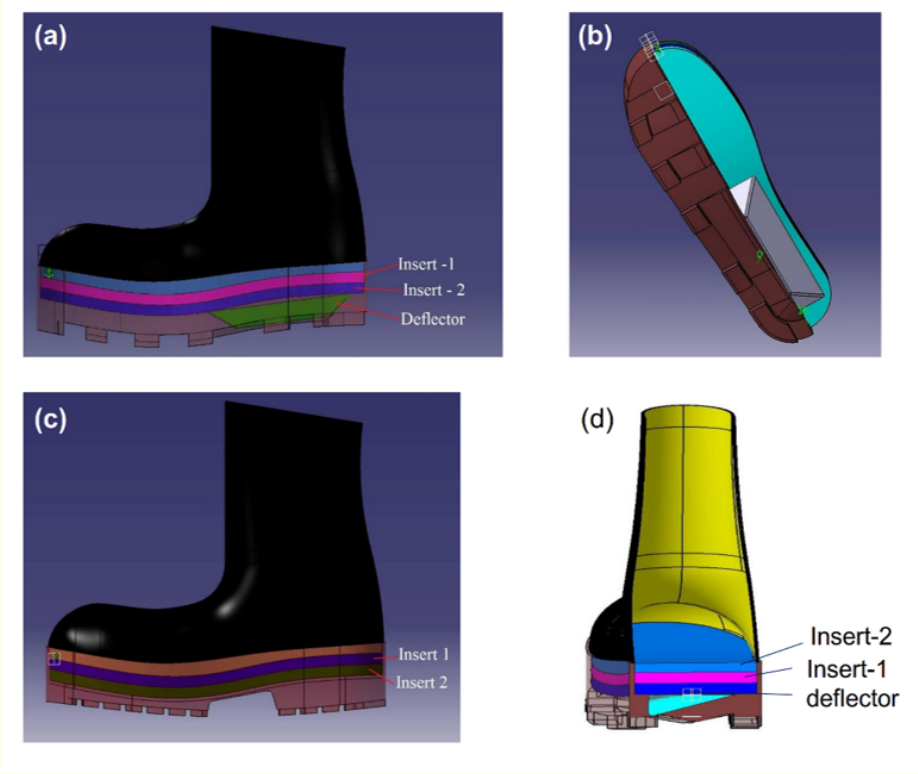

Figure 3: *Schematic views and sole view of protective boots; (a) General view of Type 2; (b) sole view of Type 2; (c) general view of Type 1 and (d) cross section view of Type 3.*

The characteristics of the boot samples used in blast tests and numerical simulations are provided in table 1. Deflector, which was used at the mentioned samples, consists of 2 mm-thick steel plates with 3 mm cell sized aluminum honeycomb used at the core. Top of the deflector was covered with a 1 mm thick steel plate after placing the honeycomb inside. The deflector is positioned near the boot's heel as the maximum damage occurs for a blast right below the heel. Sizes and schematic representations of the deflectors were given in figure 4. Properties of the deflectors and composite materials used in the sole were provided in table 1.

Sample	Sole													Upper Boot Reinforcement		
	Deflector Insert plate-1					Insert plates in the sole										
						Insert plate-2				Between leather and inter lining						
	Material	Thickness (mm)	Taper Angle (°)	Filler	Height (mm)	Material	Plate Thickness (mm)	Fabric Plies Number	Fiber Volume Fraction (%)	Material	Plate Thickness (mm)	Fabric Plies Number	Fiber Volume Fraction (%)	Material	Fabric Plies Number	Fabric weight (g/m²)
Type 1	No deflector					UD Aramid	9.5 ± 0.6	21	65	UD Aramid	9.5 ± 0.6	31	65	Aramid Woven fabric (CT 736)	2	410
Type 2	Steel	2	106	Al. Honeycomb	21	UD Aramid	9.5 ± 0.6	21	65	UD Aramid	9.5 ± 0.6	31	65	Aramid Woven fabric (CT 736)	2	410
Type 3	Steel	2	20	Al. Honeycomb	21	UD Aramid	9.5 ± 0.6	21	65	UD Aramid	9.5 ± 0.6	31	65	Aramid Woven fabric (CT 736)	2	410

Table 1: *Production parameters of boot samples.*

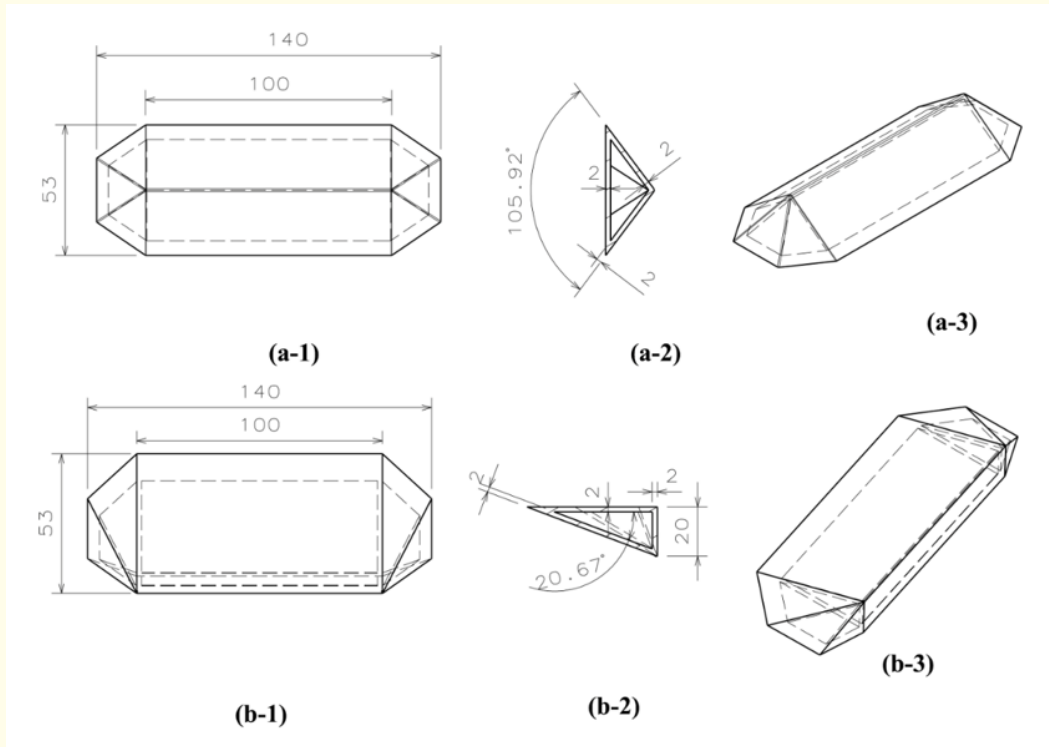

Figure 4: *Schematic views and sizes of deflectors; (a) Type 2 deflector; (b) Type 3 deflctor; 1, 2 and 3 indicate that sizes on front view, cross section and isometric view respectively.*

Aramid UD fabric, for which the properties are provided in table 2, was used as reinforcement and nolax A21.2007 low density polyethylene (LDPE) adhesive film (density 0.94 g/cm^3, melting temperature 80°-90°C and melt flow rate of 6 - 9 g/10 min) was used as a matrix system. The properties of fibers used in the preparation of reinforcing structures, are given in table 3.

Reinforcement type	Application	Reinforcement producer	Weave type	Linear density of Warp/ Fill yarns, Tex	Warp/ Fill (or 0°-90°) yarns	Thread density, threads/10 cm	Areal density, g/m^2	Crimp Warp/ Fill, %	Reinforcement thickness, mm
Aramid UD sheet- GS3000	Composite Insert	FMS	UD	126/126	Kevlar 49/Kevlar 49	-	510	Non-crimp	0.50
Aramid woven fabric- CT 736	Upper boot	Teijin	2X2 Basket weave	336/336	Twaron 2000/ Twaron 2000	127/127	410	0.8/0.8	0.6

Table 2: *Properties of reinforcements used in the study.*

Parameters	Twaron 2000® (Aramid)	Kevlar 49® (Aramid)
Young modulus, GPa	85	112
Strength, cN/Tex	235	208
Ultimate elongation, %	3.5	2.4
Density, g/cm^3	1.44	1.44

Table 3: *Parameters of the aramid fibers used in the study.*

Methodology

Numerical simulations

Explicit Finite Element Analysis was carried out using ANSYS LS-Dyna. Blast, equivalent to 54 gr TNT, was modelled using *Initial_Impulse_Mine which is based on the analytical model developed by Trambley [21]. Core of the deflector and composite layers were discretized using linear solid elements with nodal pressure, while shell elements were preferred for steel plates of the deflector (Figure 5). *Contact_Eroding_Surface_To_Surface contact algorithm was used between all parts with Soft = 1 option. Because of the efficiency issues related with explicit scheme, a continuum 3D solid element with orthotropic material model was assumed for the honeycomb instead of modelling the individual cell walls. The equivalent material properties of the solid elements were found through a separate uniaxial compression analysis along 3 coordinate axes with Aluminum shell elements. Stress – volumetric strain (Figure 6) data from the shell model was used in the orthotropic material model, "*Mat_26 Honeycomb" for the solid elements. Johnson-Cook material model was assigned to Hardened AISI 4340 cover whose parameters are given in table 4 [22].

Young's Mod. (GPa)	207	A (MPa)	792	D1	0.050
Poisson's Ratio	0.3	B (MPa)	510	D2	3.440
Heat Cap. (J.Kg^{-1}.K^{-1})	477	C	0.014	D3	-2.120
Melting Point (K)	1793	m	1.030	D4	0.002
ε_0	1	n	0.260	D5	0.610

Table 4: *Johnson-Cook material model (Mat_24) parameters of hardened AISI 4340 [22].*

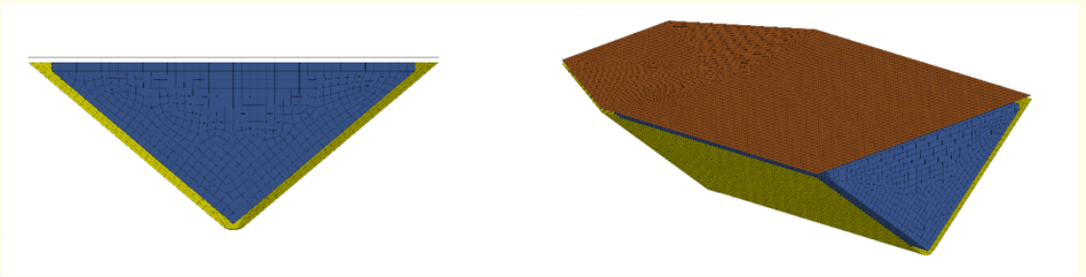

Figure 5: *FEA model used in numerical analysis. Yellow part is cover made of 4340 steel while the red part is honeycomb core.*

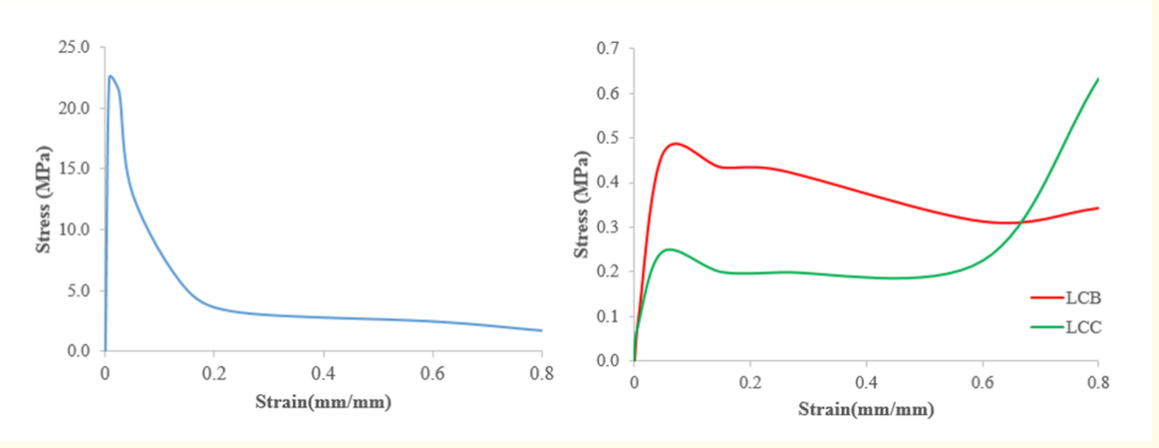

Figure 6: *Axial Stress-Volumetric Strain curves of Aluminum honeycomb calculated by a preliminary compression analysis.*

For the type 2 deflector (symmetrical tip), a total of six analyses were carried out by varying the angle, r, from 90° to 140° with 10° increments. Nodes on the top surface of the deflector were fixed with single point constraints and reaction forces were calculated for comparison.

In addition to the tip angle, separate analyses were performed for a design having asymmetrical tip (Type 3) to compare its force reduction performance with a symmetrical V-shaped (Type 2) and without any deflector (Type 1). Together with reaction forces, internal energy of the deflector was considered to investigate the energy absorption efficiency with respect to the geometry of the honeycomb (Figure 7).

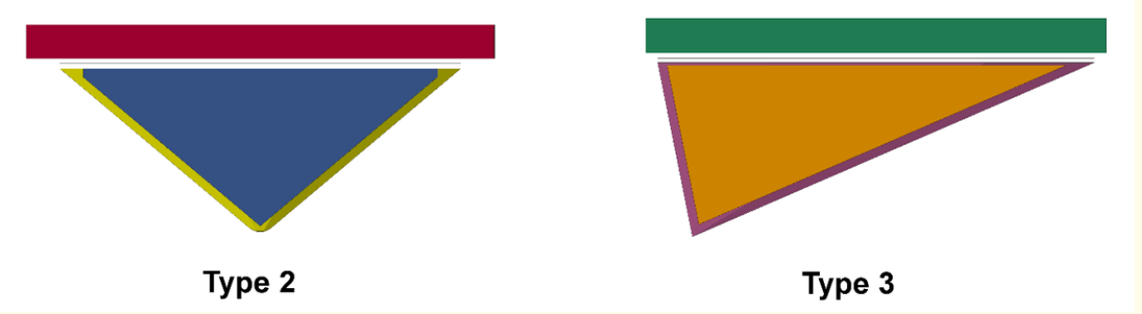

Figure 7: *Type 2 and Type 3 deflector designs. It should be noted that only wide surface of type 3 is exposed to blast loading.*

Blast tests

Blast tests were carried out using hollow frangible lower body dummies. The dummies were manufactured with 2 plies of 240 g/m^2 glass matt and polyester resin via hand lay-up method. Outer surface was covered with polyester resin based gel-coat. A wall thickness of 4mm was used throughout and the hollow volume was filled with sand to obtain a total mass of 40 kilograms. The boots were worn onto the dummies and the dummies were then tied to a metal frame which kept the dummy in standing position (Figure 8). 70 gr of TNT was used as the explosive and was placed right under and barely touching the heel of the boot. Tests were performed at the General Security Department's blast test field in Ankara. Blast tests were repeated 4 times for each deflector design.

Figure 8: *Overview of preparation of the explosion tests.*

After the blast, both the damage of the boot and of the dummy were visually inspected for qualitative comparison of the performance of different designs, as taking measurements with sensors during blast loading can be very challenging. In general, Mine Trauma Scoring (MTS) and Abbreviated Injury Scoring (AIS) are used for assessing the injuries [23]. However, the mannequin model used in this study did not allow the assessment of such injuries as the soft tissue and bones were not included in the model.

Results and Discussion

Numerical simulation results

Results of the numerical analysis with type 1 (no deflector), type 2 (symmetric V-shaped deflector) and type 3 (shifted tip) were compared in figure 9-11. Force and impulse transmitted to the composite layers and internal energy of the composite layer itself in these three cases show that the presence of the deflector is quite effective in reducing the blast loading. Without a deflector, blast loading reaches the composite layer in 5 μs (Figure 12) with a peak magnitude of 9 Mega-Newtons (Figure 9) which generates a total internal energy of 86 kJ on the composite layer. This loading was reduced to 0.37 MN (4.1%) by type 3 deflector and 0.25 MN (2.8%) by type 2.

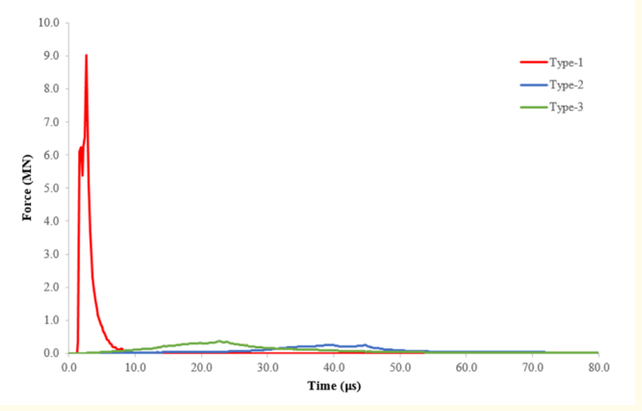

Figure 9: *Contact force vs Time graph of three types of deflectors.*

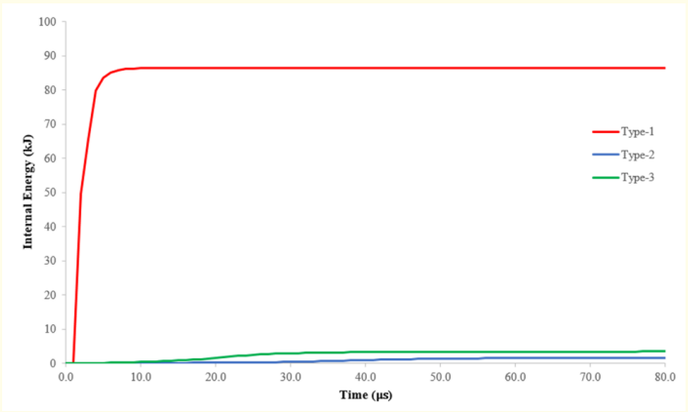

Figure 10: *Internal Energy of Composite vs Time graph of three types of deflectors.*

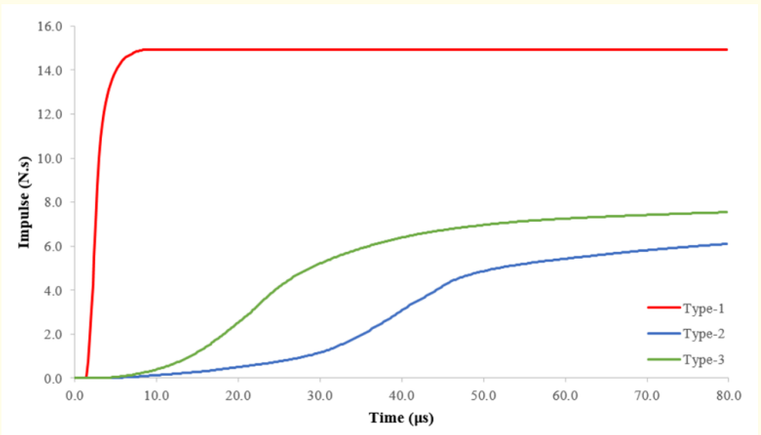

Figure 11: *Impulse acting on composite layer vs Time graph of three types of deflectors.*

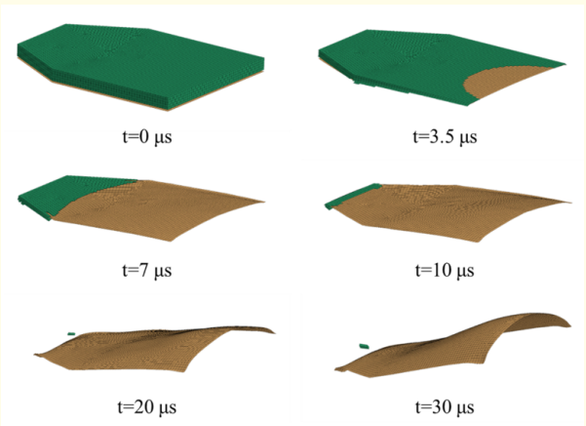

Figure 12: *Deformation of composite layer with no deflector (Type 1).*

Deformation of the deflectors, presented in figure 13 and 14, show that under the blast load honeycomb compresses significantly and composite layers were exposed to the maximum force after the honeycomb reaches the fully compacted state. Such deformation response explains the significant reduction in both the total impulse and peak force due to the deflectors. The figures also point out the difference in the geometry of deformation between type 2 and type 3 deflectors. For type 3, because of the relatively low honeycomb thickness directly above the explosion, the surface of the deflector facing the blast loading compresses and hits the upper surface of the deflector much earlier than that of type 2. This is due to the asymmetrical design of type 3, which causes a non-homogeneous compression of the honeycomb core. This argument is supported by the numerical results given in table 5 as the time of peak force is 27 μs for type 3 while it is 39 μs for type 2. Difference in the internal energy stored by the composite (Figure 10) is due to the fact that higher energy is transferred to the composite layer for type 3. It should be also noted that the angle of incidence in type 3 is lower compared to that for type 2 which causes a higher impulse acting per unit area. These results show the presence of a deflector is essential to reduce the impulsive loads transmitted to the upper parts of the boot and type 2 deflector design is much more effective than type 3 in doing so.

Boot	Composite Int. Energy (kJ)	Max. Force (MN)	Time of Max. Force (μs)	Max. Impulse (N.s)
Type-I	86.30	9.0	4	14.9
Type-II	1.52	0.254	39	6.1
Type-III	3.35	0.372	27	7.4

Table 5: *Peak values of force, impulse and internal energy.*

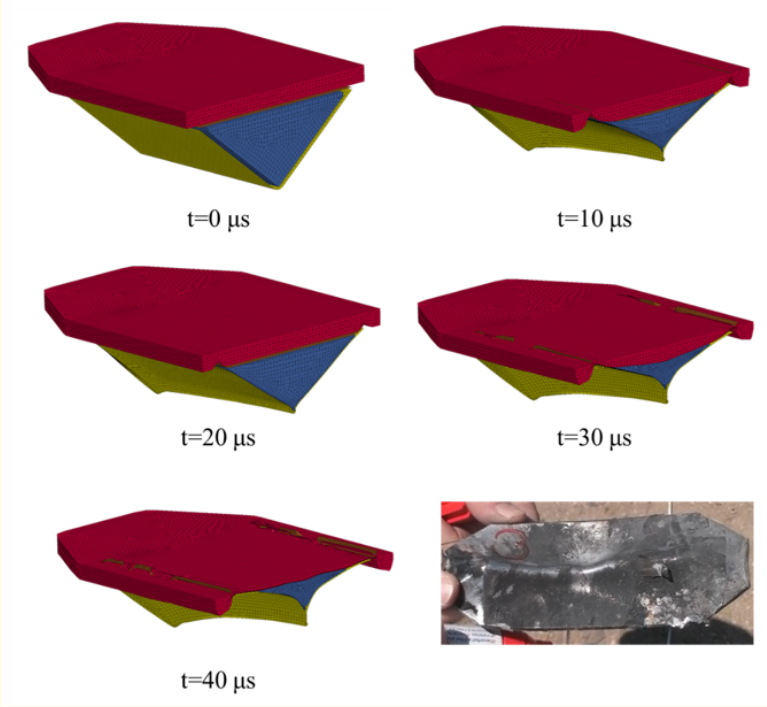

Figure 13: *Deformation of composite layer with type 2 deflector.*

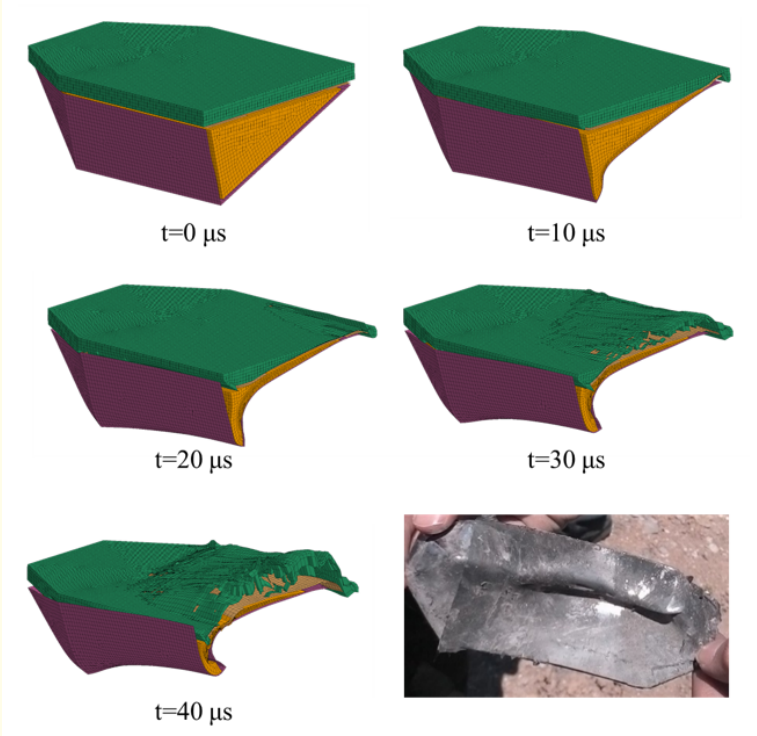

Figure 14: *Deformation of composite layer with type 3 deflector.*

Results of the numerical analysis, performed for tip angle optimization in type 2 design, are presented in figure 15. The figure shows that as the tip angle, r, increases, the reaction force, which represents transmitted force from deflector, increases. This result reveals that, within a practical tip angle range, the effect of increasing the angle of incidence governs over the combined effect of increasing surface area and decreasing standoff distance. This conclusion is further supported by the fact that a lower tip angle provides a higher core volume in the deflector which reduces the transmitted force more efficiently.

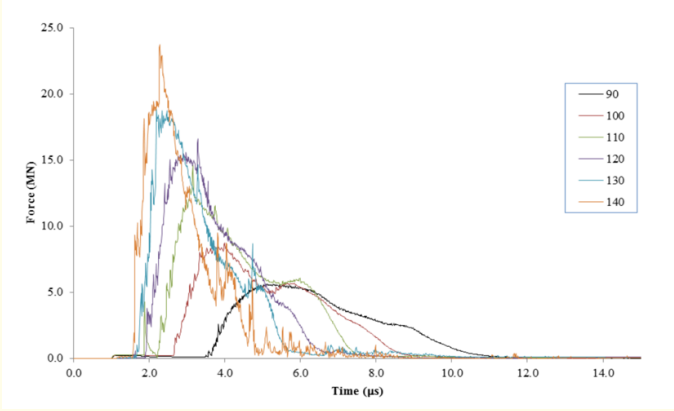

Figure 15: *Reaction force vs time result of various tip angles of type 2 deflector.*

Impulse acting on the composite layers can be obtained by integrating the force over time. Figure 16 shows that the total impulse reaches higher values for larger tip angles (low angle of incidence). At larger tip angles the total volume of core material (aluminum honeycomb) is reduced, hence limiting the energy absorbed by the inelastic deformation mechanism and transmitting higher peak forces to the upper layers.

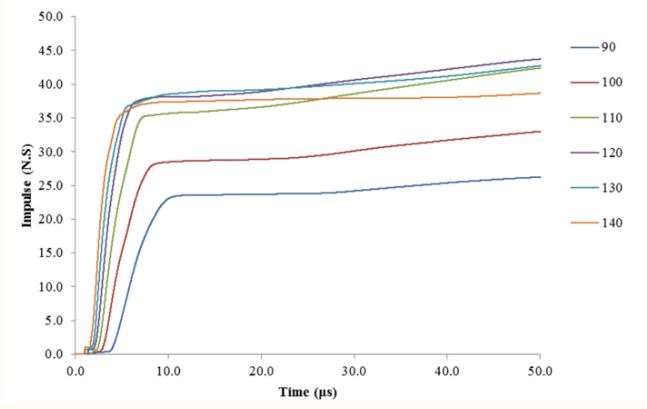

Figure 16: *Impulse vs time result of various tip angles of type 2 deflector.*

Blast test results

Blast tests were performed in order to compare the damage on the mannequin legs wearing three different sole designs. Test results for Type-1 (without deflector) boots are provided in figure 17 which reveals that the boots were torn into pieces and both feet were detached at the ankle. In addition, for all four repetitions, the upper parts of the legs, in particular knees and femurs, were severely damaged. These results show that without any deflecting or energy absorbing medium, composite layers alone are not able to reduce force transmitted to the feet which leads to fracture near the ankle being the weakest point in the lower body.

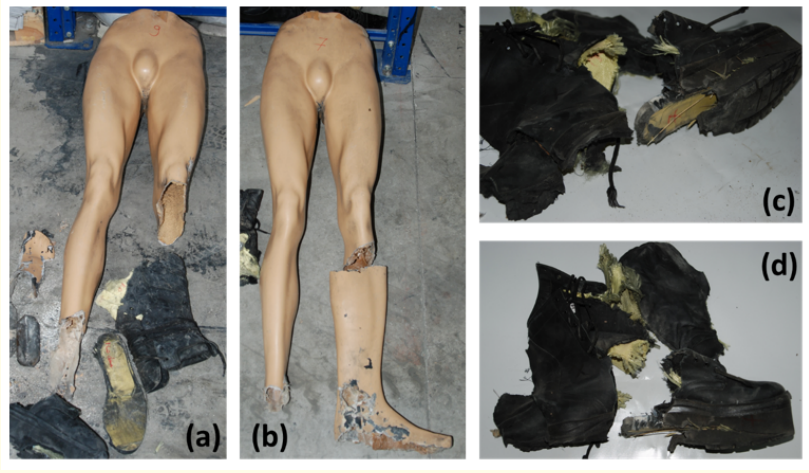

Figure 17: *View of model (a and b) and boot (c and d) after the blast test for sample Type-1.*

Blast test results of Type-2 boots, which has symmetrical V-shaped deflector, are provided in figure 18. The figure shows that, consistently on all four repetitions the damage is significantly lower than that of Type-1. Only the foot above the mine is detached and no further fracture was observed on the other ankle or in upper parts. This conclusion proves that a big percentage of the shockwave was deviated or absorbed by the deflector, hence extremely reducing the force transmitted upwards. In addition, as can be seen in Figure 18, the boot itself didn't lose much structural integrity. Only the heel of the sole was ripped, keeping all other parts intact. No serious deformation at the composite layers were observed.

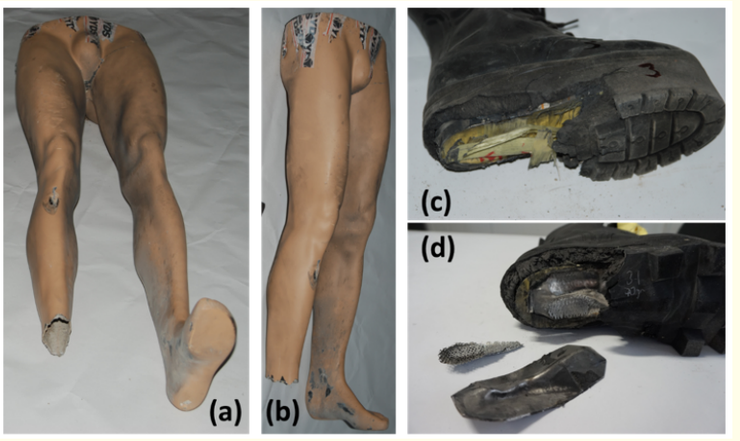

Figure 18: *View of model (a and b) and boot (c and d) after the blast test for sample Type-2.*

As a third alternative, an unsymmetrical deflector design was tested (Type-3 boots) with the tip of the deflector being closer to the other leg. The objective of such a biased tip position was to minimize the shockwave deflected in the direction of the other leg. However, according to the test results, this expectation was not fulfilled. It was observed that for Type-3 boot design both of the feet were broken from a similar location to that for type 1 boots. Nonetheless, fractures were not as severe as for type 1. On the boots' side, severe damage of the deflectors were observed. Unlike type 2, type 3 boot itself showed extreme damage both at the heel and at other parts, which is another indication they may not have enough protective property (Figure 19).

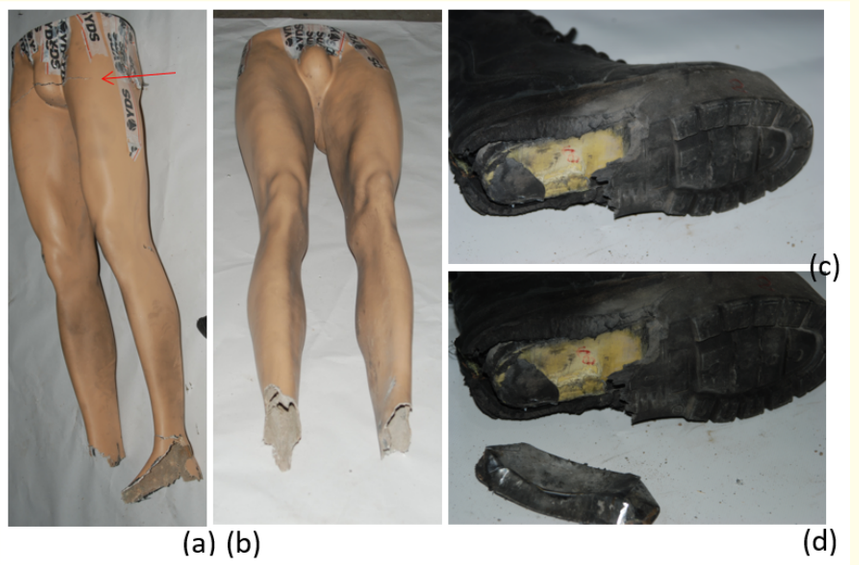

Figure 19: *View of model (a and b) and boot (c and d) after the blast test for sample Type-3.*

Conclusion

In this study, the effectiveness of the blast deflectors used in protective footwear against AP mines was investigated. The tip-angle of the V-shaped deflector and the overall shape (symmetrical, unsymmetrical) were chosen as the design parameters to be examined.

Blast analysis in LS-Dyna shows the deflectors greatly reduce the blast force transmitted to the foot and lower leg. This reduction of force is due to shock waves deflected by the inclined surfaces of the deflector and also energy absorption due to compaction of the aluminum honeycomb filling inside the deflector. When compared to the case with no deflectors, an unsymmetrical and symmetrical deflector reduced the peak force by a factor of 24 and 36, respectively.

The qualitative observations during the blast tests also confirm these conclusions. For the no deflector case (Type-1), both legs of the dummy showed extreme damage both below and above the knee. For both Type-2 (symmetrical) and Type-3 (unsymmetrical) deflectors, the damage was observed to be significantly below the no deflector case.

As an extension to the current research, the effectiveness of the composite layers above the deflector will be investigated through the optimization of design parameters such as material, lay-up and thickness.

Bibliography

1. Shariful I., *et al*. "The Spider Boot: An effective foot protective systems against anti-personnel mine blasts". *Journal of Mine Action* 4.2 (2000): 7.
2. Traverso LW., *et al*. "Combat casualties in Northern Thailand: emphasis on land mine injuries and levels of amputation". *Military Medical* 146.10 (1981): 682-685.
3. Makris A., *et al*. "Anti-Personnel mine foot protection systems, US patent no: 6.006.646" (1999).
4. Krohn HF., *et al*. "Protective footpad assembly, US patent no. 2.720.714" (1952).
5. Chavet I and Madmoni A. "Minefield shoe and method for manufacture thereof, US2003/0172554 A1" (2003).
6. Ringler S and Chavet I. "Device for reducing the danger of accidental detonation of a landmine, US patent no: 4.611.411" (1986).
7. Jordan RD. "Protective footgear, US patent no. 3.516.181" (1970).
8. Fujinaka ES., *et al*. "Blast Protective Footwear, US patent no: 3.318.024" (1996).
9. Vaz GA. "Protective boot and sole structure, US patent no: 6.425.193.B2" (2002).
10. Vaz GA. "Protective boot and sole structure, US 2002/011011 A1" (2002).
11. Vaz GA. "Protective boot and sole structure, US 2002/0011146 A1" (2002).
12. Zepf HP. "Multi-layer boot-sole has injection molded or pressed base reinforced by embedded multi-filament fibers, German patent DE 4214802" (1993).
13. Aleven AAW. "Puncture resistant insole for safety footwear, US patent no: 5.285.583 A" (1994).
14. Vaz GA. "Blast and fragment resistant safety boot footwear, US patent no: 5.979.081" (1999).
15. Joynt VP and Dyk JTV. "Protective footwear, US 2006/0000117 A1" (2006).

16. Zeman P. "Anti Land Mine-Boots, WO 03/037125 A1" (2001).

17. Lohrmann HR. "Anti-personnel mine protective footpad, US patent no: 5.992.056" (1999).

18. Peche JP., *et al*. "Appliance for protecting against the effects of explosive devices, US patent no: 6.655.051" (2003).

19. Peche JP., *et al*. "Appliance for protecting against the effects of explosive devices, WO/2000/050837" (2000).

20. Trimble K and Clasper J. "Anti-Personnel Mine Injury Mechanism and Medical Management". *Journal of the Royal Army Medical Corps* 147.1 (2001): 73-79.

21. Trembley JE. "Impulse on Blast Deflectors from a Landmine Explosion, Technical Report No: DREV – TM – 9814". Defense Research Establishment. UNCLASSIFIED (1998).

22. Johnson GR and Cook WH. "Fracture Characteristics of Three Metals subjected to Various Strains, Strain Rates, Temperatures and Pressures". *Engineering Fracture Mechanics* 21.1 (1985): 31-48.

23. Horst MJ., *et al*. "Blast performance of commercially available demining footwear: a summary of experimental trials on surrogate legs". TNO Defence, Security and Safety, Report No: TNO-DV 2008 A379 (2008).

Volume 11 Issue 4 April 2020